Spectroscopic Analysis of pH-Induced Changes in the Molecular Features of Type A Botulinum Neurotoxin Light Chain†

Li Li and Bal Ram Singh*

Department of Chemistry and Biochemistry and Center for Marine Science and Technology, University of Massachusetts, Dartmouth, Dartmouth, Massachusetts 02747

Received November 29, 1999; Revised Manuscript Received March 1, 2000

ABSTRACT: *Clostridial botulinum* neurotoxins (BoNTs) cause neuroparalysis by blocking neurotransmitter release at the neuromuscular junctions. While the toxin's heavy chain (HC) is involved in binding and internalization, the light chain (LC) acts as a unique Zn^{2+}-endopeptidase against a target protein in the exocytotic docking/fusion machinery. During the translocation of the LC to the cytosol, it is exposed to the endosomal low pH. Low pH showed a dramatic change in the BoNT/A LC polypeptide folding as indicated by differential heat denaturation. Furthermore, binding of 1-anilinonaphthalenesulfonate (ANS) revealed exposure of hydrophobic domains of BoNT/A LC at low pH. Low-pH-induced structural (and by implication the endopeptidase activity) changes were completely reversible. Exposure of BoNT/A LC to low pH (4.7) did not, however, evoke the loss of Zn^{2+} bound to its active site. Implications of these observations to the delivery of active BoNT/A LC to the nerve cell are discussed. We further analyzed the nature of low-pH-induced change in the polypeptide folding of BoNT/A LC by Trp fluorescence measurements. The Trp fluorescence peak was observed at 322 nm, and the two fluorescence lifetime components estimated at 2.1 ns (88%) and 0.6 ns (12%) did not change much at low pH. These observations suggested that the two Trp residues are buried and constrained in a hydrophobic environment, and it is likely that the core of the BoNT/A LC protein matrix does not participate in the low-pH-induced structural alteration. This conclusion was further supported by the near-UV circular dichroism spectra under two pH conditions.

Botulinum neurotoxins (BoNTs)[1] are highly potent toxins which inhibit neurotransmitter release from peripheral cholinergic synapses. The structurally related family of BoNT consists of seven different serotypes (A−G). BoNTs are synthesized as single polypeptide chains of approximately 150 kDa each, which are cleaved endogenously or exogenously resulting in a 100 kDa heavy chain (HC) and a 50 kDa light chain (LC) linked through a disulfide bond. The 150 kDa neurotoxin comprises three functional domains: the catalytic domain confined to the LC, the translocation domain in the N-terminal half of the HC, and the receptor binding domain in the C-terminal half of the HC. The mode of BoNT action involves three steps (*1*): extracellular binding and internalization, membrane translocation, and intracellular blockage of acetylcholine release. In the initial step, the neurotoxin binds to the presynaptic membrane through lipid and an as yet to be clearly identified protein receptor (*2*). The binding step is followed by endocytosis-mediated internalization. The pH inside the endosome is lowered through a proton pump, which triggers membrane pore formation by the HC by inducing exposure of the hydrophobic polypeptide segments in the N-terminal domain of the HC (*3*). The membrane pore formation allows translocation of at least the LC across the endosomal membrane (*4*). Finally, the LC domain of neurotoxin cleaves the synaptosomal protein of 25 kDa (SNAP-25) through its Zn^{2+}-endopeptidase activity, and blocks the docking and fusion of synaptic vesicles, leading to the inhibition of acetylcholine release (*5*, *6*). A major unanswered question regarding the mode of action of BoNT action is the following: How does the LC get translocated across the endosomal membrane? Also, does the endopeptidase activity remain the same after exposure to low pH in the endosome?

It has been reported that the acidic lumen of endosome induces conformational changes in the HC compatible for pore formation on the membrane (*3*, *7*, *8*). Very little is known about the mechanism by which LC translocation occurs through the lipid bilayer. The size of the pore formed by BoNT/B HC has been estimated to be about 8 Å (*9*). Such a pore is unlikely to accommodate the 50 kDa LC. It has been speculated that the low pH could unfold the LC, which could then be accommodated in the HC pore (*3*, *9*). A question remains to be answered whether the exposure to

† This work was supported in part by a grant from the National Institutes of Health−National Institute of Neurological Disorders and Stroke (NS33740) and by the U.S. Department of Agriculture (95-37207-2427). B.R.S. is a Henry Dreyfus Teacher-Scholar.

* Address correspondence to this author at the Department of Chemistry and Biochemistry, University of Massachusetts, Dartmouth, 285 Old Westport Rd., Dartmouth, MA 02747. Phone: 508-999-8588. Fax: 508-999-8451. E-mail: bsingh@umassd.edu.

[1] Abbreviations: BoNT/A, *Clostridium botulinum* type A neurotoxin; HC, heavy chain of BoNT; LC, light chain of BoNT; SNAP-25, synaptosomal-associated protein of 25 kDa; ANS, 1-anilinonaphthalene-8-sulfonate; DTT dithiothreitol; IPTG, isopropyl β-D-thiogalactopyranoside; Tris, tris(hydroxymethyl)aminomethane; SDS−PAGE, sodium dodecyl sulfate−polyacrylamide gel electrophoresis; CD, circular dichroism.

10.1021/bi992729u CCC: $19.00
Published on Web 05/03/2000

acidic pH provokes any conformational change of the LC, and if it does, whether the conformational changes are reversible to maintain the endopeptidase activity. Since the endopeptidase activity of the LC inside the cytoplasm is relevant only after its exposure to the low pH, it is important to compare enzymatic activity before and after exposure to the low pH.

In this study, we have examined the structure and the enzymatic activity of BoNT/A LC under neutral and low-pH conditions, and the reversibility of these parameters after exposure to different pH conditions. Results indicate that the structure and activity of the LC are reversible after low-pH exposure, and low-pH conditions induce exposure of hydrophobic segments of BoNT/A LC, a feature relevant for its translocation through endosomal membrane.

MATERIALS AND METHODS

All common reagents used were obtained from Sigma Chemical Co. (St. Louis, MO), and were of the highest grade available. ANS was purchased from Molecular Probes (Eugene, OR). All the solutions were made in deionized distilled water.

Purification of Recombinant Proteins. Expression of wild-type and mutant LC was induced by IPTG for 15 h at 30 °C. The recombinant LC had six histidine residues tagged at the C-terminal end. LC from *E. coli* extract was purified on a Ni^{2+} column followed by DEAE-A50 chromatography, as described previously (*10*). Purity of the LC preparation was confirmed by a single band on an SDS−PAGE (sodium dodecyl sulfate−polyacrylamide gel electrophoresis) gel during the final purification step. The endopeptidase activity of His-tagged recombinant LC is identical to the BoNT/A activity (*10*). All the following experiments were performed in 20 mM Tris, pH 7.0, containing 50 mM NaCl. LC samples for the study of pH effect were prepared by dialysis against the same buffer at a given pH. To check the pH-induced reversibility of LC structure and activity, the LC sample was brought back to neutral pH after treating with low pH, i.e., sequential dialysis of the protein against pH 4.6 and then against pH 7.0 buffer.

Endopeptidase Assay. The enzymatic activity of LC was assayed by monitoring the decrease in the band intensity of SNAP-25 on an SDS−PAGE gel. The SNAP-25 digestion experiments were carried out by incubating 20 μM SNAP-25 (human SNAP-25a) with 20 nM BoNT/A LC in a 10 μL volume at 37 °C for varying incubation periods, between 5 and 30 min. The low-pH-treated LC was prepared as described above. The buffer used for the cleavage reaction was 20 mM Tris, pH 7.0, containing 50 mM NaCl and 1 mM DTT (dithiothreitol). The cleavage reaction was terminated by addition of SDS−PAGE sample buffer to the mixture. The products were resolved by electrophoresis on a 10% polyacrylamide gel with a constant running voltage set at constant 110 V, for better resolution. The gel was stained with Coomassie blue, and scanned for integrating the band density using an *itti* Imager (itti, I.c., St. Petersburg, FL). To determine the initial rate of SNAP-25 cleavage, the intact SNAP-25 band was integrated for density in respective lanes with different concentrations of SNAP-25 used in the reaction mixture, and compared with the integrated density of the control SNAP-25 (without LC). Since the amount of cleaved SNAP-25 product is relatively small during the initial reaction period used for estimating initial rates, the corresponding band on SDS−PAGE is relatively faint compared to the intact SNAP-25 band. Therefore, we chose to estimate the reaction rates based on a decrease in the amount of intact SNAP-25.

UV and Circular Dichroism Spectroscopy. Optical absorbance spectra were recorded with a Jasco (model V550) spectrophotometer using a 1.0 cm path length quartz cuvette. The specific absorbance coefficient was calculated to be ϵ_{280}(LC) = 0.83 mg^{-1} cm^{-1} using a protein concentration based on BCA protein assay (*11*).

Circular dichroism (CD) spectra were recorded at 4 °C with a Jasco J715 spectropolarimeter. The cuvettes used for far-UV and near-UV CD spectral recordings had path lengths of 0.1 and 1.0 cm, respectively. The scan speed was 20 nm min^{-1}, and the response time was fixed at 8 s. LC samples in the range of 0.1−0.3 and 0.5−1.0 mg/mL were used for far-UV and near-UV CD measurements, respectively. In the near-UV CD region, a total of four scans were recorded and averaged to increase the signal-to-noise ratio. In all CD experiments, the buffer blank was recorded separately and subtracted from the sample spectrum. Mean residue weight ellipticities were calculated by using a molecular mass of 52.67 kDa for the LC. On the basis of amino acid sequence, the mean residue weight was calculated to be 113.81. The secondary structure calculation was carried out by SELCON using the Softsec program (Softwood Co.).

Thermal denaturation studies were performed by monitoring the CD signal at 217 and 280 nm using 0.1 and 0.5 cm path length cuvettes, respectively. Temperature was raised at a rate of 2 °C/min from 30 to 100 °C. In a parallel experiment, entire far-UV or near-UV CD spectra were recorded every 2 °C during the temperature ramping between 30 and 100 °C.

Fluorescence Measurement. Steady-state Trp fluorescence and fluorescence lifetime data were recorded on an ISS K2 (Champaign, IL) multifrequency cross-correlation phase and modulation fluorometer equipped with polarizers. As per needs, the instrument was switched between the steady-state mode, with or without the polarizers engaged, and the lifetime mode. The fluorescence spectra were recorded with the excitation wavelength fixed at 295 nm. The excitation and emission slits were set to 8 nm. To minimize the inner filter effect, the sample concentration was fixed such that the absorbance at 295 nm (excitation wavelength) was less than 0.1. The reference and protein (2−4 μM) samples in a 1.0 cm path length cuvette were placed in a water-jacketed cuvette holder maintained at a constant temperature of 4 °C.

Trp fluorescence lifetime measurements were carried out using the phase-modulation method. The excitation wavelength was set at 295 nm, and emission was measured using a 335 nm cutoff filter in the emission path. For the Trp fluorescence lifetime measurements, the fluorescence of terphenyl dissolved in ethanol was used as a reference. The AC/DC signals from the reference compound (*p*-terphenyl) and protein sample were adjusted to approximately the same value, before the actual measurements were made. Twelve frequencies were used between 2 and 200 MHz in the log mode, with a minimum of 5 and a maximum of 10 measurements at each frequency. The phase angle shifted

between 0 and 90°, and the modulation varied between 0 and 1.0. The residuals for the phase angles were within ±1.5, and for the demodulation, these were within ±0.02. The lifetimes were calculated using both the phase shift and demodulation data using software provided by ISS (Champaign, IL). Data were fit using frequency-independent errors of 0.2° for the phase and 0.02 for the modulation. We used the two-component model to fit the observed data which provided the best fit as judged from the lowest χ^2 values.

Urea Denaturation of LC. A stock solution (2 mg/mL) of LC prepared in dialysis buffer (20 mM Tris, 50 mM NaCl, 1 mM DTT, pH 7.3) was diluted to a fixed protein concentration of 0.3 mg/mL by a combination of 10 M urea and dialysis buffer in various ratios to yield final urea concentrations between 0 and 8 M. Samples were microcentrifuged, and fluorescence lifetime measurement was performed as described above.

ANS Binding. Interaction of the fluorescence dye ANS (1-anilinonaphthalene-8-sulfonate; Molecular Probes, Eugene, OR) with LC at different pHs was analyzed by measuring the fluorescence emission of the protein-bound dye. ANS was dissolved in absolute ethanol, and its concentration was determined spectrophotometrically [ϵ_{372}(ANS) = 8000 M^{-1} cm^{-1}]. One microliter aliquots of 0.8 mM ANS were added into a 1 cm path length cuvette containing 2 mL of 1 μM protein solution. Final ethanol concentrations in the protein samples were kept below 1% (v/v). The samples were gently mixed for 1 min at 10 °C using a stirring bar. For fluorescence measurement, the excitation wavelength was fixed at 370 nm. Excitation and emission slits were set to 8 and 2 nm, respectively. The fluorescence intensities were estimated by averaging 10 readings of the emission at 480 nm taken during a 15 s monitoring period. The final fluorescence intensity at any given ANS concentration was derived after correcting for the dilution effect and the blank signal of ANS fluorescence in the absence of the protein. Control experiments of ANS fluorescence in the absence of protein were conducted in the same way as described above.

Zinc Content. For zinc analysis, the protein samples were extensively dialyzed against 20 mM Tris buffer (pH 7.0 or pH 4.7) containing 50 mM NaCl in metal-free dialysis tubing prepared as suggested by Fu et al. (*12*). The concentration of residual zinc in the buffer was subtracted from those in the targeted protein samples. Graphite furnace atomic absorption spectrometry was utilized for zinc analysis. Absorbance peaks by both methods were measured at 213.9 nm. All values shown are averages of duplicate determinations. The detection limit for zinc was 1.5 nM.

RESULTS

Secondary Structure. The CD spectrum of LC dissolved in 50 mM Tris, pH 7.0, containing 50 mM NaCl displayed the characteristic double minimum at 208 and 220 nm expected of a α-helix-rich protein (Figure 1A). LC dissolved in 20 mM Tris, pH 4.6, containing 50 mM NaCl exhibited a far-UV CD spectrum identical to that at neutral pH (Figure 1A).

Tertiary Structure, Circular Dichroism, and Steady-State Fluorescence. Near-UV CD and intrinsic tryptophan fluorescence emission spectroscopies were employed to examine the topography of aromatic amino acid residues. The near-UV CD spectrum between 250 and 310 nm of BoNT/A LC is shown in Figure 1B. The CD spectrum of LC consists of a well-defined negative band at 280 nm, which can be ascribed to the tyrosine residues (*13*). A shoulder was observed at 270 nm, which can be attributed to the phenylalanine residues (*12*, *13*). There was no significant CD signal at 290−300 nm. BoNT/A LC has two tryptophan residues: W43 and W118. Although we observed absence of a band in the 285−300 nm region associated with the tryptophan signal, a small shoulder could be visualized at ∼285 nm. A hidden band at 286 nm was resolved by using the second derivative of the spectrum (Figure 1B, bottom) and could be ascribed to tryptophan. It is possible that the small Trp signal at 286 nm is overshadowed by the large Tyr signal at 280 nm, resulting in the absence of a distinct Trp peak. Upon exposure of LC to the pH 4.6 buffer, the near-UV CD

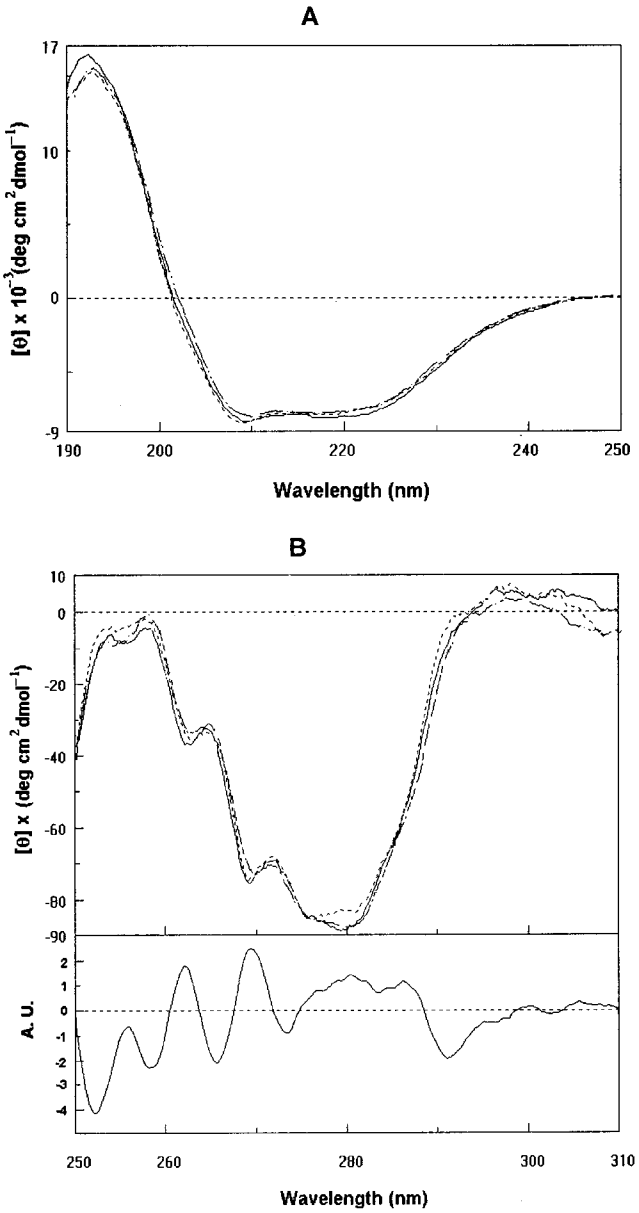

FIGURE 1: Near-UV (A) and far-UV (B, top) circular dichroism spectra of BoNT/A LC at pH 7.0 (solid curve), pH 4.6 (dotted curve), and reversed pH 7.0 (dashed curve) in the far-UV region. The second derivative of the spectrum (B, bottom), which corresponds to LC at pH 7.0, was used to resolve a hidden peak at 286 nm.

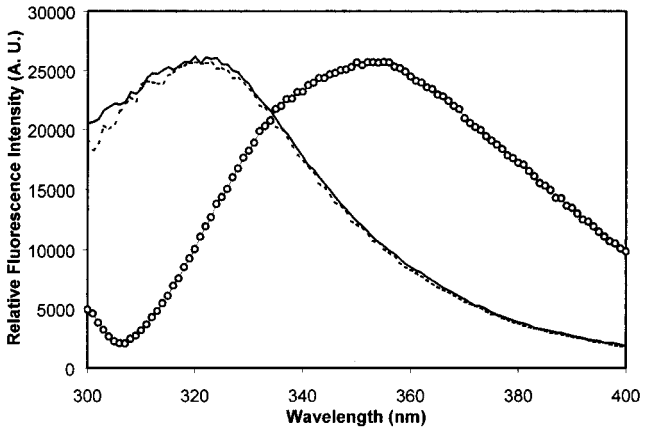

FIGURE 2: Fluorescence emission spectra of free tryptophan (circles) and of LC at neutral pH (solid curve) and acidic pH (dotted curve). The LC was dissolved in 20 mM Tris, 50 mM NaCl, maintained at either pH 7.0 or pH 4.7. Spectral recordings were carried out at 10 °C. Excitation wavelength was set at 295 nm. The absorbance at 295 nm was less than 0.1 for LC dissolved in both the pH 7.0 and 4.7 buffers.

Table 1: pH Effect on Lifetimes of Tryptophan in BoNT/A LC[a]

	f_1	τ_1	f_1	τ_2	χ^2
pH 7.0	0.88	2.12 ± 0.15	0.12	0.60 ± 0.10	4.1
pH 4.6	0.85	2.31 ± 0.10	0.15	0.74 ± 0.15	4.6
Re-pH 7.0	0.91	2.23 ± 0.12	0.09	0.46 ± 0.09	3.8

[a] Excitation wavelength 295 nm.

spectral features remained virtually unchanged, except for the signal at 280 nm. The negative CD band at 280 nm shifted to 277 nm due to a small but reproducible loss of signal at 280 nm (Figure 1B). This observation suggests that the microenvironment or flexibility of polypeptide segments containing one or more Tyr residues is altered with lowering of the pH to 4.6. The CD signal change at 280 nm was reversible (Figure 1B), further supporting the real nature of the structural changes introduced by the pH.

LC displayed a fluorescence emission maximum at approximately 322 nm with excitation at 295 nm. The excitation at 295 nm selectively excites Trp residues. The significantly blue-shifted emission maximum of Trp fluorescence in LC, compared to free tryptophan, suggests that its two tryptophan residues are located in a hydrophobic environment of protein matrix. No difference was observed when the fluorescence emission peaks of LC at neutral and acidic pH were compared (Figure 2).

Fluorescence Lifetime. The microenvironment around the tryptophan residues was assessed by estimating the fluorescence lifetimes of the tryptophan residues in LC. Both phase angle change and demodulation data recorded as a function of modulation frequency were adequately fitted for a two-component decay of the Trp fluorescence, as indicated by the low chi square value for the curve fitting. The two lifetime components of Trp fluorescence were calculated to be 2.12 ± 0.15 and 0.60 ± 0.10 ns (Table 1). The existence of two widely different lifetimes for the two Trp residues indicated the presence of two distinct environments for these residues in LC, which may arise either from their distinct locations in the protein molecule or from a dynamic conformation of the polypeptide in the vicinity of the Trp residues. Two possible factors could account for the shorter

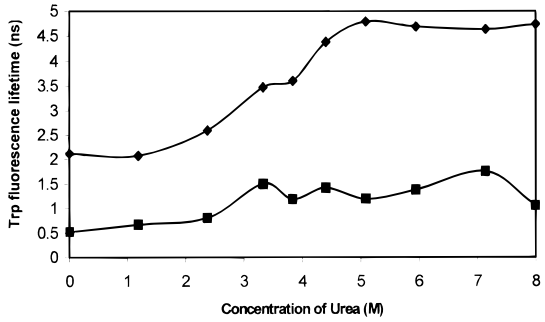

FIGURE 3: Urea denaturation of LC as monitored by tryptophan fluorescence lifetime. Samples were prepared as described under Materials and Methods. The increased lifetime values in the unfolded state suggest that the tryptophan residues have quenched fluorescence lifetime by nearby residues in the native state.

Table 2: Secondary Structure Estimation of LC (pH 4.7) at Different Temperatures

temp (°C)	% α-helix	% β-sheet	% turns	% random coil
25	27	17	20	36
100	26	31	15	28

lifetime of the Trp residue: exposure to the polar aqueous surroundings or close proximity to an intrinsic quencher moiety within the protein core of the LC. To distinguish these two possibilities, urea denaturation monitored by Trp fluorescence lifetime was examined. Upon unfolding of the protein with increase of urea concentration, both Trp fluorescence lifetime values increased (Figure 3). The longer lifetime component shifted from 2.1 to 4.7 ns while the shorter lifetime component changed from 0.5 to ~1.2 ns. The increased lifetimes in denatured LC are due to the removal of intrinsic quenching by protein unfolding. These data suggest that the Trp residues are buried in the protein core with quenched fluorescence lifetime by nearby residues in the folded state.

Trp fluorescence lifetimes of LC at neutral and acidic pH were virtually indistinguishable (Table 1), indicating the microenvironments of the two Trp residues remained similar under the two pH conditions.

Temperature Denaturation. To probe the pH effect on LC stability, thermally induced unfolding of LC was examined by monitoring the CD signals at 217 and 280 nm as a function of temperature. Figures 4 and 5 show the thermal transition curves of LC under different two pH conditions. The unfolding curves of LC dissolved in pH 7.0 buffer, and that of LC at pH 7.0 after being exposed to pH 4.7 buffer, obtained from CD recordings in the far- and near-UV regions, coincide and indicate a T_m (the first derivative of the melting curves was calculated for a more accurate determination of T_m) value of 52 °C (Figure 4). Both the secondary (217 nm; Figure 4) and tertiary structures (280 nm; Figure 5) unfolded simultaneously at pH 7.0 irrespective of whether the LC had been pretreated with low pH.

While temperature-induced alteration in the structure of LC at pH 7.0 leads to a decrease in the CD signal in both far- and near-UV regions, heating of LC at pH 4.7 unusually showed an enhanced CD signal at 217 nm (Figure 4, top and bottom right). We noticed a heat-induced conformational rearrangement of α-helix to β-sheet dominant state in the LC structure (Table 2). This heat-resistant β-sheet structure was retained up to 100 °C. A relatively small signal change

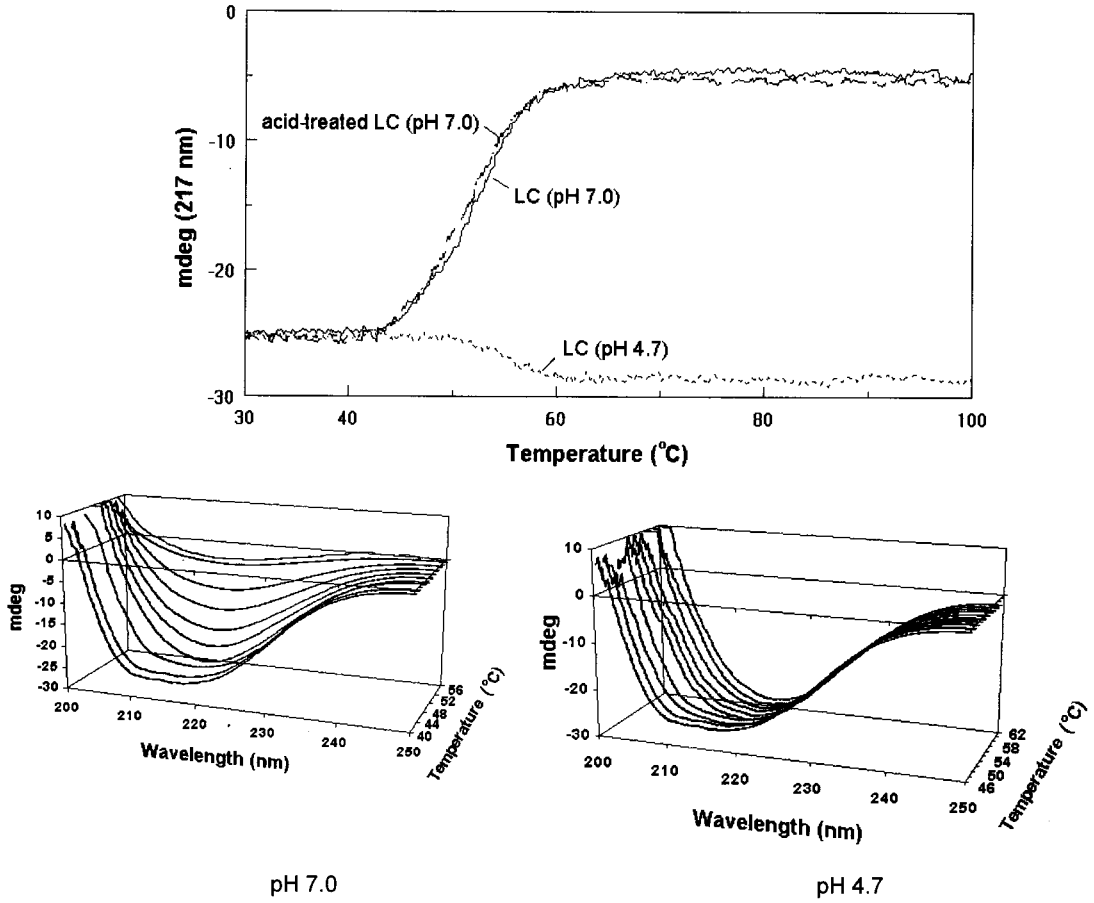

FIGURE 4: Top panel: Temperature-dependent unfolding of LC at pH 7.0 and pH 4 as monitored by the far-UV circular dichroism band at 217 nm. Bottom panels: pH effect on the far-UV CD spectra of LC at different temperatures during the structural transition at 2 °C intervals. Left panel, pH 7.0; right panel, pH 4.7. mdeg (millidegree) is the unit of ellipticity.

(−25 to −28°) and a low signal-to-noise ratio in $\Delta[\theta]$ (change in ellipticity) precluded accurate estimates of the apparent midpoint of the transition from the unfolding curve of LC at pH 4.7 (Figure 4). However, when the thermal stability was monitored by the CD signal at 280 nm, it showed an unfolding with a T_m of 52 °C (Figure 5). Notably, a considerable amount of residual tertiary structure seems to have been retained in LC at pH 4.7 even at 100 °C, in contrast to a total loss in LC at pH 7.0. The thermal stability of LC at different pHs showed very a distinct pattern, suggesting different protein foldings under these two conditions. The heat-induced structural change of LC at both pHs was irreversible. The irreversibility might be attributed to the protein aggregation observed upon heating.

Since LC under both pH conditions remained stable up to 40 °C, estimation of the secondary structure at 25 °C represents the native structure of the LC. Table 2 lists alterations in the secondary structure content of LC at low pH with respect to temperature change. The data indicate that the α-helix content remained unchanged and the turn content was marginally affected by the temperature. An appreciable enhancement in the β-sheet content is observed, which appears to be at the expense of β-turns and random coils (Table 2).

ANS Binding. ANS has been used as a general probe for solvent-exposed hydrophobic clusters (*14*, *15*). Proteins with poorly packed interiors typically have a high affinity for ANS, the binding of which can be monitored spectroscopically (*15*). We characterized ANS binding properties of LC at pH 7.0 and 4.7. The binding of the apolar dye ANS to LC is associated with an enhanced fluorescence and a blue shift in the wavelength of the maximum emission from 515 to 480 nm (Figure 6 inset). LC at neutral pH displayed high affinity for ANS. However, there is a more substantial increase in the fluorescence intensity when ANS binds to the LC at pH 4.7 than at pH 7.0 (Figure 6). In a control experiment, the ANS fluorescence in the absence of protein showed very small variation with pH. Thus, acidic pH appears to induce conformational changes in the LC which cause an exposure of the hydrophobic surface of the protein. ANS has been widely used to detect the formation of molten globule-like intermediates in the folding pathways of several proteins (*16*). The molten globule state is characterized to be as compact as the native protein with solvent-accessible hydrophobic regions and an appreciable amount of secondary structure but no rigid tertiary structure (*17*). The substantial enhancement in the ANS fluorescence intensity upon its binding to the LC at low pH indicates additional accessibility of the LC hydrophobic surface or cavity to ANS. Such features are characteristics of ANS binding to protein with a molten globule state.

Enzymatic Activity. The above results suggested the pH-induced overall structural change is reversible. To investigate whether this reversibility is physiologically significant, a comparison of the endopeptidase activity of LC before and after treatment with low pH was performed (Figure 7). The

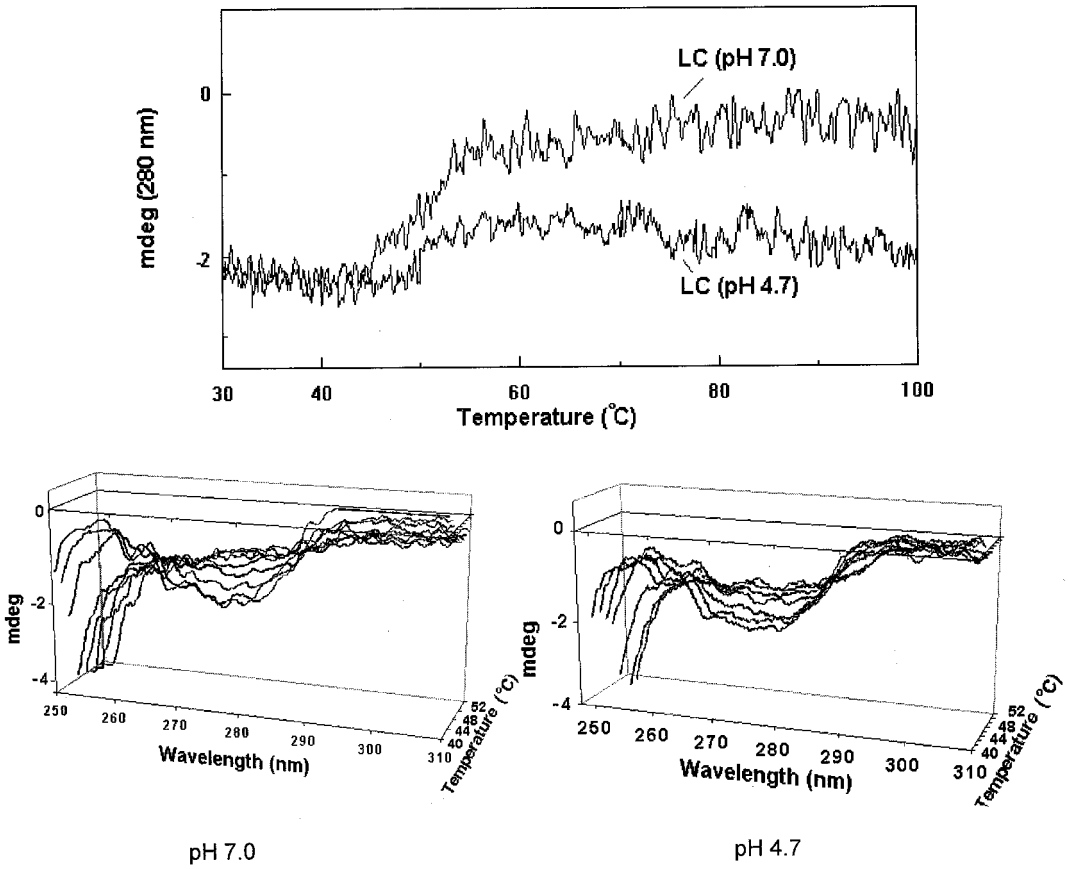

FIGURE 5: Top panel: Temperature-dependent unfolding of LC at pH 7.0 and pH 4.7 as monitored by the near-UV circular dichroism band at 280 nm. Bottom panels: pH effect on the near-UV CD spectra of LC at different temperatures during the structural transition (from 40 to 52 °C) at 2 °C intervals. Left panel, pH 7.0; right panel, pH 4.7.

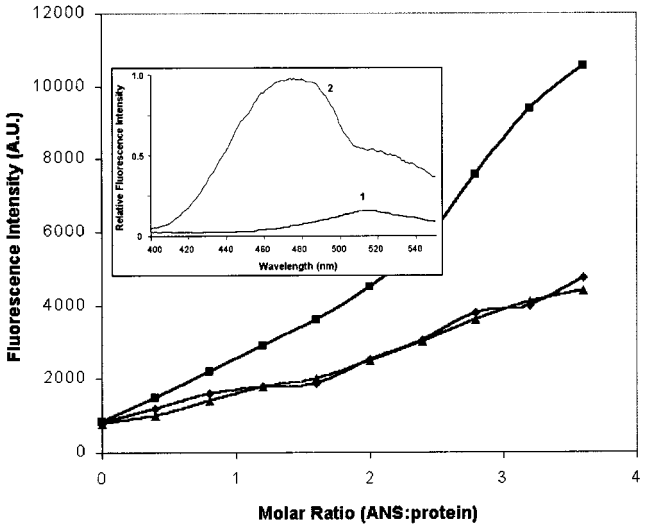

FIGURE 6: ANS binding to LC at pH 7.0 (triangles) and pH 4.7 (squares) and reversibility of pH effect on ANS binding (diamonds). 1 μL aliquots of ANS (stock = 0.8 mM in ethanol) were added to 2 mL LC samples (1 μM), and the fluorescence intensity was measured at 480 nm with excitation at 370 nm. ANS fluorescence intensity was plotted against the molar concentration of ANS. Inset: curve 1 represents the fluorescence emission of LC in the absence of ANS with excitation at 370 nm; curve 2 represents the fluorescence emission spectrum of LC in the presence of ANS.

specific enzymatic activities of two forms of LC were virtually identical.

Zinc Content. The purified recombinant proteins were analyzed for Zn^{2+} content using graphite furnace atomic absorption spectrometry. Previous studies, including the X-ray crystallography analysis, have suggested a single Zn^{2+} residue at the BoNT/A active site (*18*−*20*). In our analysis, we confirmed earlier reports and estimated one Zn^{2+} per BoNT/A LC molecule. This observation is relevant to the use of recombinant BoNT/A LC for understanding the structure−function relationship of BoNT/A. The recombinant LC has a His hexamer tagged at the C-terminal end of the LC and does not seem to capture any extra Zn^{2+}. Exposure of the LC to low pH did not cause release of the Zn^{2+} (Table 3), as could be expected from a protonated form of the protein.

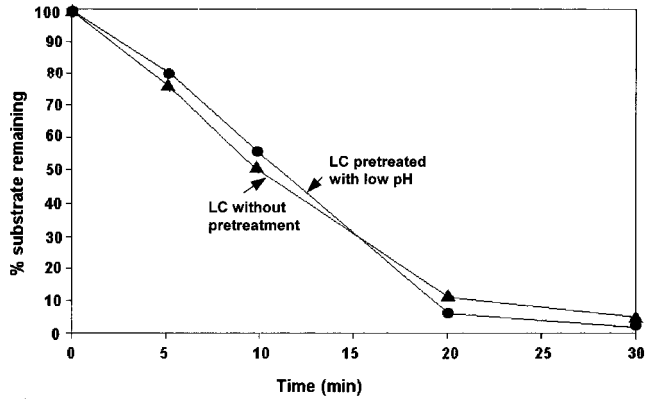

FIGURE 7: Endopeptidase activity of LC before and after low-pH treatment. 20 μM SNAP-25 was incubated with 20 nM LC at 37 °C for different periods of incubation. Reaction was terminated by addition of SDS−PAGE sample buffer, and uncleaved SNAP-25 was estimated by densitometry.

Table 3: Zinc Content in LC at pH 7.0 and pH 4.7

LC	Zn^{2+} (mol/mol of protein)
pH 7.0	1.1 ± 0.2
pH 4.7	1.2 ± 0.3

DISCUSSION

Light chain of botulinum neurotoxin is the catalytic domain that fully accounts for its toxicity. The crystal structure of the entire toxin is available at 3.3 Å (*18*). An intriguing discovery made in the crystal structure reveals that an unusual belt consisting of the N-terminal peptide segment of the HC wraps around the LC. The belt is attached to the LC through a disulfide bond. Interestingly, reduction of the disulfide bond between light and heavy chains is required for expression of the BoNT/A Zn^{2+}-endopeptidase activity in vitro (*19*, *20*). This is perhaps associated with the release of the light chain from the grip of the HC belt, which leads to activation of the BoNT/A endopeptidase activity. The dynamic conformation of the separated LC, therefore, seems to be critical for its enzymatic activity, and warrants examination in detail.

CD analysis and intrinsic fluorescence emission spectroscopy indicate that the LC possesses a defined set of secondary and tertiary structures. The two Trp residues are in a hydrophobic environment as indicated by a blue-shifted emission λ_{max} of 322 nm. Such an observation would indicate that these residues are perhaps buried deep inside the protein matrix of BoNT/A LC. However, a nearly nonexistent CD signal corresponding to Trp residues (Figure 1B) was an intriguing observation, as a buried Trp residue should exhibit a strong CD signal in the near-UV region. Two possible explanations can account for the featureless near-UV CD signal of Trp residues. (i) In the case of a real absence of the CD signal in the 285−300 nm region, the Trp residues are likely to be located in a highly flexible segment of the protein. (ii) The actual Trp signal is not observed because of a relatively large negative Tyr peak observed at 280 nm right next to the 285−300 nm region, and the expected Trp signal is covered in the tail of the Tyr peak. To resolve a possible hidden peak, a second derivatization of the near-UV CD spectrum was carried out. A positive second-derivative peak at 286 nm was observed (Figure 1B), indicating a significant CD signal contribution perhaps by the Trp residues. Previously, the 286 nm CD signal has been assigned to Trp residues (*13*, *20*). This information, along with the Trp fluorescence data, allowed us to conclude that the Trp residues in BoNT/A LC are constrained in the protein hydrophobic core, a feature supported by the recently released X-ray crystal structure of BoNT/A (*18*).

Even though a significant CD band was identified at 286 nm corresponding to the Trp residues of BoNT/A LC, its strength is weaker than its expected strength in BoNT/A holotoxin comprised of the L and H chains (*13*). The absence of a CD signal corresponding to the ^1L_b transition at 295 nm indicates the existence of an asymmetric microenvironment with respect to only the ^1L_a transition of the Trp residues. In BoNT/A, where both the L and H chains are joined together through a disulfide bond, the CD signals corresponding to both ^1L_a and ^1L_b transitions are enhanced. Interestingly, reduction of the disulfide bond in BoNT/A yields a near-UV CD spectrum which resembles the composite (by mathematical addition) of the CD spectra of separated L and H chains (*13*, *20*). As pointed out earlier, reduction of the disulfide is required for the endopeptidase activity of BoNT/A (*13*, *20*). Thus, the Trp topography of BoNT/A LC could be severely altered in the active (disulfide bond reduced) BoNT/A endopeptidase, which seems to coincide with the purified BoNT/A LC.

In an effort to characterize the Trp topography of BoNT/A LC further, Trp fluorescence lifetimes were estimated. The two lifetimes observed for Trp fluorescence are relatively short (2.1 and 0.6 ns; Table 1) compared to free Trp, or Trp which is exposed to solvent (*21*). Such a short Trp fluorescence lifetime is indicative of a strong quenching of the excited state by intrinsic quencher, either through proximal (primary structure) or through distal (polypeptide folding) mechanisms. This observation is consistent with an earlier report which showed the Trp fluorescence quantum yield of BoNT/A LC as 0.07 (*22*). A survey of the primary structure of the BoNT/A light chain shows that Trp-43 has fluorescence quenching amino acid residues His-39, Lys-41, and Glu-47 in its vicinity, whereas Trp-118 does not have any such residues located around it (*23*, *24*, and references cited therein). The X-ray crystal structure has revealed additional quenching groups such as Lys-37, Arg-145, and Glu-147, which are within 7 Å distance of Trp-43 (*18*). The side chain of His-39, although pointing away from Trp-43, is still within 8 Å distance of Trp-43. Quenchers within approximately 10 Å radius of Trp could have a significant effect on its fluorescence (*25*). In the case of Trp-118, only two quenching groups, Lys-128 and Glu-148, are in its vicinity (*18*). We therefore assign the short-lifetime component (τ_2) to Trp-43 and the long-lifetime component (τ_1) to Trp-118. To confirm the distal nature of the intrinsic fluorescence quenching of Trp-118, we denatured BoNT/A LC with urea, and monitored changes in the Trp fluorescence lifetime (Figure 3). An increase in the long-lifetime component of the Trp fluorescence (τ_1) from 2.1 to 4.7 ns suggests a strong folding-dependent intrinsic quenching of the Trp fluorescence, as predicted from the X-ray structure (vide supra). The short-lifetime component (τ_2) did not exhibit a dramatic change in the fluorescence lifetime, confirming our conclusion that this component is likely to arise from Trp-43, which has several vicinal quenching groups. Since Trp residues of BoNT/A LC appear to undergo considerable topographical changes for its activation either after chain separation or after disulfide bond reduction (*13*, *20*, *22*), the information on their fluorescence lifetime identification with individual Trp residues will help decipher the role of different polypeptide segments in its unique endopeptidase activity.

In the proposed mode of BoNT/A action, BoNT/A LC is exposed to low-pH conditions inside endosomes before being translocated into the cytosol where the substrate for its endopeptidase activity is available (*3*, *26*). A question has remained whether the exposure of the LC to low pH affects its structure and endopeptidase activity. Exposure of the LC to low pH was associated with a dramatic change in its polypeptide folding, as revealed by distinctly different temperature-induced unfolding patterns (Figure 4). However, the pH-induced change in the BoNT/A LC is completely reversible, as indicated not only by reversal of the polypeptide unfolding pattern but also by the identical endopeptidase activity of BoNT/A LC before and after exposure to low

pH (Figure 7). In view of these results, in vivo enzymatic studies of BoNT/A LC carried out without its prior exposure to low pH should be entirely relevant to in vivo conditions where the LC gets exposed to low pH.

The unfolding of BoNT/A LC at pH 7.0 and 4.7 (Figure 4) exhibited an intriguing pattern in that it did not lose its secondary structure even at 100 °C. The secondary structure content itself remained identical for BoNT/A LC dissolved in pH 7.0 and 4.7 buffers (Figure 1A) at 25 °C. However, at 55 °C, while the secondary structure was almost completely lost in BoNT/A LC at pH 7.0, the secondary structure was fully retained in BoNT/A at pH 4.7 (Figure 4). However, a shift in the CD signal band to 217 nm in BoNT/A LC at pH 4.7 indicated a shift in the secondary structural folding from a α-helix dominating protein to a *β*-sheet dominating BoNT/A LC protein at and above 55 °C. Retention of secondary structure under protein denaturing temperature conditions has been interpreted as the presence of a molten globule structure (*27*). The presence of a molten globule structure at low pH could represent a very significant observation in view of the suggested mechanism of BoNT/A L translocation across endosomal membrane through a membrane channel formed by the BoNT/A H chain (*3*, *9*, *28*, *29*).

The H chain of BoNT is shown to form a membrane channel with a pore size of 8 Å or less (*9*, *29*, *30*). In order for the 50 kDa BoNT LC to translocate across the membrane, it has been speculated that the LC becomes unfolded at low pH to allow a single-strand chain to pass through the narrow channel formed by the H chain (*30*). While the observation of a molten globule is not entirely consistent with the prediction of an unfolded structure of BoNT/A LC, the existence of a molten globule structure could provide the flexibility needed in the process of BoNT/A LC passage through a presumably narrow BoNT/A H chain membrane channel. Since the pH-induced conversion of the native structure of BoNT/A LC into a molten globule structure could become a defining event in its translocation across the endosomal membrane, we decided to further confirm the existence of such a structure at low pH.

One of the ways to test the presence of molten globule structure is by examining its binding with a nonpolar dye, ANS (*16*). A molten globule structure allows ANS to access the hydrophobic segments of the protein, which results in the enhancement of the dye's fluorescence. In our experiments with BoNT/A LC, the ANS fluorescence increased considerably more upon binding with BoNT/A LC at pH 4.7 than at pH 7.0 (Figure 6). Although ANS binding suggests the possibility of a molten globule structure, we decided to further confirm the existence of a molten globule structure by monitoring the topography of Tyr residues.

The existence of a molten globule structure is monitored by observing a change in the structural folding in the same temperature range where the secondary structure remains intact. We monitored Tyr topography change as a function of temperature by recording the CD signal at 280 nm. Although the decrease in the CD signal was smaller in BoNT/A LC at pH 4.7 than at pH 7.0, the transition occurred at an identical temperature (Figure 5). Such an observation suggests a similar flexibility in polypeptide folding of BoNT/A LC under the two pH conditions. In a molten globule state, generally a tertiary structure transition occurs at a lower temperature than the secondary structure transition. A contrary observation (Figure 5) clearly suggests that the low-pH BoNT/A LC may not be a typical molten globule structure.

Less than clear data on the existence of a typical molten globule structure of BoNT/A LC at pH 4.7 warrant another explanation of the experimental observations. It seems low pH introduces two types of structural changes in BoNT/A LC: (I) the structure (especially the secondary structure) becomes resistant to change, reflecting rigidity in polypeptide folding; (II) enhanced binding of ANS, indicating exposure of hydrophobic groups of BoNT/A LC. Exposure of hydrophobic groups could allow its interaction with the lipid bilayer, an observation that has been experimentally confirmed previously (*31*, *32*). The rigidity of the structure may be the result of interaction of exposed hydrophobic groups with the solvent. Since Trp residues appear to be located in the hydrophobic regions of the protein matrix, and there is little change in their spectral characteristics at two pHs (Figures 2 and 4; Table 1), the hydrophobic groups involved in the interaction with ANS at low pH are likely to be located toward the surface of the protein matrix. These results suggest that the translocation of the BoNT/A LC may occur through a mechanism other than the membrane channel formed by the BoNT/A H chain. In a "cleft model" proposed initially for diphtheria toxin, and later adapted for BoNT, the interaction of the BoNT/A LC directly with lipid bilayer has been envisaged (*3*, *33*). Further experiments are needed to confirm this mechanism.

In conclusion, we have characterized the structure of BoNT/A LC in terms of its Tyr and Trp topography. The Trp topography appears to be important in the active endopeptidase structure of BoNT/A LC. Low pH induces exposure of hydrophobic segments of BoNT/A LC which introduces rigidity in the secondary as well as the tertiary structure of the BoNT/A LC. These observations support the "cleft model" of membrane structure for BoNT/A LC translocation.

REFERENCES

1. Simpson, L. L. (1986) *Annu. Rev. Pharmacol. Toxicol. 26*, 427−453.
2. Schengrund, C. L. (1999) *J. Toxicol. Toxin Rev. 18*, 35−44.
3. Lebeda, F. J., and Olson, M. A. (1994) *Proteins: Struct., Funct., Genet. 20*, 293−300.
4. Stecher, B., Gratzl, M., and Ahnert-Hilger, G. (1989) *FEBS Lett. 248*, 23−27.
5. Montecucco, C., and Schiavo, G. (1993) *Trends Biochem. Sci. 18*, 324−327.
6. Li, L., and Singh, B. R. (1999) *Toxin Rev. 18*, 95−112.
7. Beise, J., Hahnen, J., Andersen-Beckh, B., and Dreyer, F. (1994) *Naunyn Schmiedebergs Arch. Pharmacol. 349*, 66−73.
8. Lebeda, F. J., and Singh, B. R. (1999) *J. Toxicol. Toxin Rev. 18*, 45−76.
9. Hoch, D. H., Romero-Mira, M., Ehrlich, B. E., Finkelstein, A., DasGupta, B. R., and Simpson, L. L. (1985) *Proc. Natl. Acad. Sci. U.S.A. 82*, 1692−1696.
10. Li, L., and Singh, B. R. (1999) *Protein Expression Purif. 17*, 339−344.
11. Smith, P. K., Krohn, R. I., Hermanson, G. T., Mallia, A. K., Gartner, F. H., Provenzano, M. D., Fujimoto, E. K., Goeke, N. M., Olson, B. J., and Klenk, D. C. (1985) *Anal. Biochem. 150*, 76−85.
12. Fu, F. N., Lomneth, R. B. Cai, S., and Singh, B. R. (1998) *Biochemistry 37*, 5267−5278.

13. Singh, B. R., and DasGupta, B. R. (1989) *Biophys. Chem. 34*, 259−267.
14. Slavik, J., Horak, J., Rihova, L., and Kotyk, A. (1982) *J. Membr. Biol. 64*, 175−179.
15. Semisotnov, G. V., Rodionova, N. A., Razgulyaev, O. I., Uversky, V. N., Gripas, A. F., and Gilmanshin, R. I. (1991) *Biopolymers 31*, 119−128.
16. Ptitsyn, O. B. (1995) *Adv. Protein Chem. 47*, 83−229.
17. Ptitsyn, O. B., Pain, R. H., Semisotnov, G. V., Zerovnik, E., and Razgulyaev, O. I. (1990) *FEBS Lett. 262*, 20−24.
18. Lacy, D. B., Tepp, W., Cohen, A. C., DasGupta, B. R., and Stevens, R. C. (1998) *Nat. Struct. Biol. 5*, 898−902.
19. Schiavo, G., Rossetto, O., Santucci, A., DasGupta, B. R., and Montecucco, C. (1992) *J. Biol. Chem. 267*, 23479−23483.
20. Cai, S., Sarkar, H. K., and Singh, B. R. (1999) *Biochemistry 38*, 6903−6910.
21. Beechem, J. M., and Brand, L. (1985) *Annu. Rev. Biochem. 54*, 43−47.
22. Singh, B. R., and DasGupta, B. R. (1989) *Mol. Cell. Biochem. 85*, 67−73.
23. Binz, T., Kurazono, H., Wille, M., Frevert, J., Wernars, K., and Niemann, H. (1990) *J. Biol. Chem. 265*, 9153−9158.
24. Gryczynski, I., Eftink, M., and Lakowicz, J. R. (1988) *Biochim. Biophys. Acta 954*, 244−252.
25. Eftink, M. R., and Ghiron, C. A. (1981) *Anal. Biochem. 114*, 199−227.
26. Simpson, L. L. (1981) *Pharmacol. Rev. 33*, 155−188.
27. Ptitsyn, O. B. (1995) *Trends Biochem. Sci. 20*, 376−379.
28. Singh, B. R. (1996) *Adv. Exp. Med. Biol. 391*, 63−84.
29. Montal, M. S., Blewitt, R., Tomich, J. M., and Montal, M. (1992) *FEBS Lett. 313*, 12−18.
30. Oblatt-Montal, M., Yamazaki, M., and Montal, M. (1995) *Protein Sci. 4*, 1490−1497.
31. Montecucco, C., Schiavo, G., Gao, Z., Bauerlein, E., Boquet, P., and DasGupta, B. R. (1988) *Biochem. J. 251*, 379−383.
32. Montecucco, C., Schiavo, G., and Dasgupta, B. R. (1989) *Biochem. J. 59*, 47−53.
33. Menestrina, G., Schiavo, G., and Montecucco, C. (1994) *Mol. Aspects Med. 15*, 79−193.

BI992729U